

Sequences within both the 5' untranslated region and the *Gag* gene are important for efficient encapsidation of Mason–Pfizer monkey virus RNA

Russell D. Schmidt,^a Farah Mustafa,^b Kathy A. Lew,^a Mathew T. Browning,^a
and Tahir A. Rizvi^{a,b,*}

^a *The University of Texas M.D. Anderson Cancer Center, Department of Veterinary Sciences, Bastrop, TX 78602, USA*

^b *Department of Medical Microbiology, Faculty of Medicine and Health Sciences (FMHS), The United Arab Emirates University, Al Ain, UAE*

Received 23 July 2002; returned to author for revision 14 October 2002; accepted 21 November 2002

Abstract

It has previously been shown that the 5' untranslated leader region (UTR), including about 495 bp of the *gag* gene, is sufficient for the efficient encapsidation and propagation of Mason–Pfizer monkey virus (MPMV) based retroviral vectors. In addition, a deletion upstream of the major splice donor, SD, has been shown to adversely affect MPMV RNA packaging. However, the precise sequence requirement for the encapsidation of MPMV genomic RNA within the 5' UTR and *gag* remains largely unknown. In this study, we have used a systematic deletion analysis of the 5' UTR and *gag* gene to define the *cis*-acting sequences responsible for efficient MPMV RNA packaging. Using an in vivo packaging and transduction assay, our results reveal that the MPMV packaging signal is primarily found within the first 30 bp immediately downstream of the primer binding site. However, its function is dependent upon the presence of the last 23 bp of the 5' UTR and approximately the first 100 bp of the *gag* gene. Thus, sequences that affect MPMV RNA packaging seem to reside both upstream and downstream of the major splice donor with the downstream region responsible for the efficient functioning of the upstream primary packaging determinant.

© 2003 Elsevier Science (USA). All rights reserved.

Keywords: Retroviruses; RNA; Beta retroviruses; Packaging; Type D; Encapsidation; MPMV; Packaging signal; Retroviral vectors; Transduction

Introduction

Viral genomic RNA encapsidation or packaging into retroviral particles is of interest because of its role in the study of the retrovirus life cycle as well as for the development of retroviral vectors. Retroviruses contain two copies of single-stranded RNA genome in each virion (reviewed in Swanstrom and Wills, 1997). These RNA genomes, which are non-covalently dimerized, must be recognized by the proteins of the assembling virion. Packaging of the viral genomic RNA is highly specific to ensure that only the

full-length, unspliced RNA is packaged as opposed to spliced viral or cellular mRNAs. This specificity is determined by the interaction of the viral Gag polyprotein and *cis*-acting sequences in the viral genomic RNA such as the packaging signal (ψ).

The Gag polyprotein, specifically the nucleocapsid (NC) region, is responsible for recognition of the viral genomic RNA (reviewed in Lever, 2000). The nucleocapsid region, which is cleaved into a separate protein upon maturation, possesses zinc finger-like domains, which are the critical elements for the recognition of the viral packaging signal (De Guzman et al., 1998; Lee et al., 1998). Indeed, mutations of these domains may lead to an abolishment of RNA packaging.

The second component of packaging, ψ , is located in the 5' region of the RNA and usually encompasses sequences

* Corresponding author. Department of Medical Microbiology, Faculty of Medicine and Health Sciences, The United Arab Emirates (UAE) University, P. O. Box 17666, Al Ain, UAE. Fax: +971-3-767-1966.

E-mail address: tarizvi@uaeu.ac.ae (T.A. Rizvi).

between the 5' untranslated region (UTR)¹ and the start of the Gag open reading frame (ORF) (reviewed in Lever, 2000; Linial and Miller, 1990). These sequences typically form secondary RNA structures in the form of stem loops. It is these stem loops and the primary sequence within them that interact with the NC region of the Gag polyprotein to confer specific viral RNA packaging. In addition, the 5' major splice donor (SD) is often near the ψ and may help the virion to preferentially select full-length unspliced viral RNA over spliced viral mRNA (Kaye and Lever, 1999).

The packaging signals of the alpha (α) retroviruses such as Rous sarcoma virus (RSV), gamma (γ) retroviruses such as murine leukemia virus (MLV), and lentiviruses such as human immunodeficiency virus (HIV) have been studied extensively (Adam and Miller, 1988; Arnoff et al., 1993; Banks et al., 1998; Banks and Linial, 2000; Bender et al., 1987; Katz et al., 1986; Lever, 2000; Linial and Miller, 1990; Mann et al., 1983; McBride and Panganiban, 1996, 1997; Rizvi and Panganiban, 1993; Watanabe and Temin, 1982 and references therein). Information gleaned from these studies has allowed the generation of retroviral vectors that have subsequently been used to define various aspects of retroviral life cycle such as the identification of retroviral receptors (Albritton et al., 1989; Takeuchi et al., 1992), strand switching during reverse transcription (Panganiban and Fiore, 1988), intracellular transport of viral RNAs (Rizvi et al., 1996a, b, 1997), etc., as well as vectors for gene delivery into target cells (Akkina et al., 1996; Mitraphanous et al., 1999; Rosenberg et al., 1990). Study of the packaging determinant of retroviruses has revealed that typically the ψ of α and γ retroviruses lies downstream of the primer binding site (PBS) and often contains a portion of *gag* gene (Linial and Miller, 1990). For these retroviruses, the packaging signal seems to be discrete and well-defined; however, in the case of the complex retroviruses such as HIV-1, HIV-2, and bovine and human T cell leukemia viruses (BLV/HTLV), the packaging signal seems to be spread out and multipartite (Mansky and Wisniewski, 1998; McBride and Panganiban, 1996; McCann and Lever, 1997; reviewed in Lever, 2000).

In contrast to these viruses, limited research has been done on delineating the sequences responsible for packaging of the beta (β) retroviruses. β -Retroviruses include viruses that display either type-B or type-D morphology during the assembly and maturation stages of virus replication, such as mouse mammary tumor virus (MMTV), Mason–Pfizer monkey virus (MPMV), and simian retroviruses (SRV). Viral vectors based on β -retroviruses are being developed to study basic steps in virus replication unique to

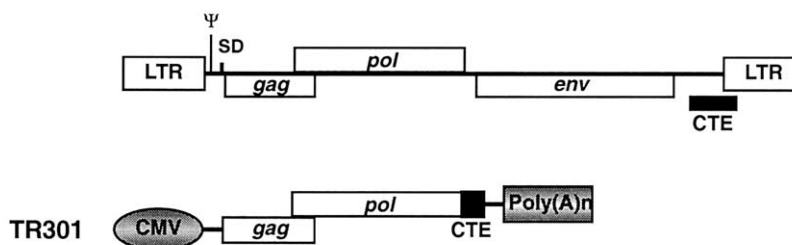
these viruses (Guesdon et al., 2001; Gunzberg et al., 1995; Li et al., 2001). In addition, such vectors may turn out to be valuable for gene therapy as well since these viruses have their own characteristics which may provide better alternatives to the existing retroviral vectors which are based on oncogenic retroviruses such as MLV or lentiviruses such as HIV (Temin, 1989). This is especially true since we have shown earlier that even phylogenetically more distantly related lentiviruses such as HIV and simian immunodeficiency virus (SIV) and feline immunodeficiency virus (FIV) can cross-package each other's genomic RNAs and propagate the RNAs for further steps in viral life cycle (Browning et al., 2001). However, a nonlentivirus similar to MPMV cannot package or propagate lentiviral RNAs even though it may be a primate retrovirus (Browning et al., 2001).

MPMV is a classical type-D retrovirus that causes an immunodeficiency syndrome in newborn rhesus monkeys (Bryant et al., 1986; Fine et al., 1975). Retroviruses very similar to MPMV that also cause AIDS in primates have been characterized such as SRV-1 and -2 (Daniel et al., 1984; Desrosiers et al., 1985; Marx et al., 1984). Among the β -retroviruses, MPMV is perhaps the most well-studied in terms of packaging and transduction. In one of the earliest such studies, a 624-bp region downstream of the PBS was shown to confer efficient packaging on MPMV-based retroviral vectors (Vile et al., 1992). Using biochemical probing, free-energy estimations, and phylogenetic analyses, part of this region (the first ~275 bases) was later shown to assume a higher order complex structure composed of eight stem loops (Harrison et al., 1995). A further limited deletion analysis of the 5' UTR of MPMV genome has shown that removal of a small 61-bp region upstream of the major splice donor reduces packaging efficiency of a replication-competent virus to 58% of the wild-type (Guesdon et al., 2001). Along the same lines, the packaging signal of a similar serogroup 2 β -retrovirus, SRV-2, has been mapped to a considerable 305-bp region at the 5' end of the viral genome (Li et al., 2001). This region contains the last 149 bp of the 5' UTR and first 156 bp immediately downstream of the *gag* ATG. However, no systematic study of the 5' end of the viral genome has been performed to characterize the nature of the packaging signal that exists within MPMV or the relative contribution of sequences with the 5' UTR and *gag* toward encapsidation.

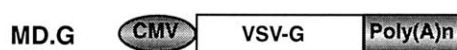
In this study, we performed a detailed deletion analysis of the 5' UTR and the *gag* gene of MPMV to delineate the minimum sequences responsible for efficient RNA packaging. Our results reveal that the packaging determinants of MPMV are complex. The primary packaging determinant exists immediately downstream of the PBS, but its efficient function is dependent upon the existence of a secondary determinant located within the 5' UTR and *gag* boundary. Thus, similar to complex retroviruses, MPMV packaging signal seems to be discontinuous, yet interdependent, with sequences important in packaging found both upstream and downstream of the major SD.

¹ Abbreviations used: CFU, colony forming units; CTE, constitutive transport element; Hyg^r, hygromycin resistant colonies; LTR, long terminal repeat; ORF, open reading frame; PBS, primer binding site; PPT, polypurine tract; SD, splice donor; SV-40, simian virus type 40; UTR, untranslated region; VSV-G, vesicular stomatitis virus glycoprotein.

A. MPMV GENOME & PACKAGING CONSTRUCT



B. ENVELOPE EXPRESSION CONSTRUCT



C. MPMV TRANSFER VECTOR

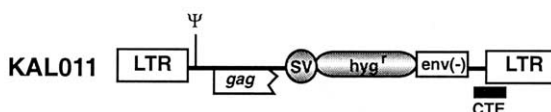


Fig. 1. Components of the MPMV in vivo packaging and transduction assay. (A) MPMV genome followed by the MPMV packaging construct, TR301. (B) The vesicular stomatitis virus (VSV) envelope glycoprotein (G) expression construct, MD.G, used to pseudotype virions expressed by TR301 containing the transfer vector RNA. (C) MPMV-based transfer vector, KAL011, used to generate the deletion mutants used in this study. CMV, cytomegalovirus promoter/enhancer; ψ , packaging signal; SD, splice donor; SV, simian virus 40 early promoter; *hyg^R*, *hygromycin B phosphotransferase* gene; CTE, constitutive transport element from MPMV.

Results

Design and construction of the in vivo packaging and transduction assay

To map the MPMV sequences involved in efficient packaging, we used our previously developed in vivo packaging and transduction assay that was used to study cross-packaging among retroviruses (Browning et al., 2001). This assay consisted of a packaging construct, TR301, which expresses the MPMV Gag/Pol proteins from the human cytomegalovirus (hCMV) promoter (Fig. 1A). Since TR301 lacks the packaging signal, RNA expressed from TR301 cannot be packaged into nascent virions. MD.G, the envelope expression vector, provided the second structural component in this assay from the vesicular stomatitis virus (VSV) (Fig. 1B). The envelope glycoprotein of VSV (VSV-G) was expressed from the hCMV promoter and allowed the newly formed virions to infect the target cells

efficiently, enabling the study of steps involved in packaging and propagation of the transfer vector RNAs. The packaging substrate in this assay was provided by KAL011, a vector that contains the entire 5' MPMV UTR (128 bp) as well as 284 bp of *gag* (Fig. 1C). In addition, it expresses the hygromycin resistance gene from the SV40 promoter (SV-Hyg^R) as a marker for successful transduction into the target cells. KAL011 can be efficiently packaged and propagated by MPMV proteins in the *trans*-complementation assay (Browning et al., 2001).

The in vivo packaging and transduction assay allowed the biological testing of mutations introduced into the transfer vectors since the defective nature of the virions produced limited the assay to a single round of replication only. Thus, the number of Hyg^R colonies observed in this assay correlated directly with the packaging efficiency of the transfer vector RNA unless other sequences involved in vector RNA propagation were affected by these mutations, such as steps involved in reverse transcription and integration. To ensure

that effects of the mutations on packaging were being scored, we also analyzed the amount of RNA packaged by the nascently produced virions directly.

The first 15 bp downstream of the PBS and the last 23 bp of the MPMV 5' UTR are important for efficient RNA packaging

To determine the role of MPMV sequences in packaging within the 5' UTR, we modified KAL011 to create a series of transfer vectors that contained varying amounts of the 5' UTR in the presence of 284 bp of *gag* (Fig. 2A). TR302 contains only the PBS, while each consecutive vector thereafter contained increasing amounts of the 5' UTR in 15 bp increments from the PBS until 105 bp in TR309. TR302–309 were tested in the *in vivo* packaging and transduction assay for the ability of transfer vector RNAs to be packaged and propagated by the MPMV proteins. This was accomplished by cotransfection of each of the transfer vectors along with the packaging construct, TR301, and the VSV-G Env expression vector, MD.G., into African green monkey kidney Cos cells. Virus was isolated 3 days posttransfection and processed for virions RNA and proteins, as well as used to infect the HeLa CD4⁺ target cells. The transfected Cos cells were processed for intracellular transfer vector RNA, while the infected target cells were selected with hygromycin B to distinguish successfully transduced cells by the appearance of hygromycin resistant colonies (Hyg^r) 10 days postinfection.

As a first step, we analyzed the relative levels of virions produced in each of the transfected cultures. Western blot analysis of virions purified from the supernatants of the transfected cultures revealed that similar levels of virions were produced in each of the transfected cultures (Fig. 2B, panel IV). Next, we analyzed the amount of RNA packaged by these virions using slot blot analysis and a radiolabeled hygromycin gene fragment as the probe (Fig. 2B, panel III). To control for RNA loading, diluted RNAs from transfected Cos cells were analyzed by slot blots using a radiolabeled β -actin probe (Fig. 2B, panel I). In parallel, a duplicate blot of cellular RNA was probed with radiolabeled hygromycin gene fragment to analyze the stability and steady-state levels of transfer vector RNAs and to estimate the transfection efficiencies (Fig. 2B, panel II). Optical densities observed in each of the slot blots were quantitated using a density analysis software, and values obtained from the analysis of RNA packaged into virions were then normalized to those obtained from cellular RNAs (see Materials and methods for details). After normalization, these analyses revealed that lack of the last 23 bp of the 5' UTR had an adverse effect on RNA packaging, leading to a 6.1-fold loss in packaging efficiency compared to the control vector, KAL011 (see TR309, Fig. 2B, panel III). The packaging efficiency remained essentially similar for the next five transfer vectors that shortened the 5' UTR from 105 to 15 bp (TR307–303). However, deletion of 15 bp of the 5' UTR

immediately following the PBS lead to an additional 2.5- to 4-fold decrease in vector RNA packaging compared to TR307–303. Relative to KAL011, this represented a 10-fold reduction in packaging efficiency (see TR302, Fig. 2B, panel III). These data reveal that the first 15 bp of the 5' UTR just downstream from the PBS and the last 23 bp are important for efficient MPMV RNA packaging, while sequences in between these extremes do not affect MPMV RNA packaging significantly.

Despite the reduction in packaging efficiency observed with the 5' UTR deletion vectors, most of the transfer vectors were successfully transduced into the target cells, leading to the generation of hygromycin-resistant colonies (Fig. 2A). However, unlike with packaging, a consistent loss in the number of Hyg^r was observed with each incremental deletion of the 5' UTR until none were observed with TR302, the vector that contains only the PBS (Fig. 2A). Lack of colonies upon transduction of TR302 was expected since PBS is required for reverse transcription of the transfer vector RNA, a step critical in vector RNA propagation. However, loss of the last 53 bp of the 5' UTR resulted in a big 17 ± 2 -fold loss in viral titers (see TR307 and TR309) with the next few deletions reducing viral titers to an eventual 1340 ± 408 -fold in 3- to 6-fold increments compared to KAL011 (Fig. 2A). These observations suggest that, in addition to packaging, the 5' UTR deletions also affected sequences involved with other steps in vector RNA propagation such as reverse transcription, integration, etc., especially the last 53 bp of the 5' UTR.

The first 100 bp of gag are sufficient for efficient RNA packaging in the presence of the entire 5' UTR

We next determined the role of *gag* sequences, if any, in the MPMV RNA encapsidation process. Toward this end, we created another series of transfer vectors that contained the entire 5' UTR (128 bp) in the presence of incremental additions of *gag*, from 30 bp in TR310 to 797 bp in KAL010 (Fig. 3A). These vectors were tested in the *in vivo* packaging assay along with the control vector, KAL011.

Analysis of viral particles produced by the packaging vector, TR301, in each of the transfected cultures revealed that most of the cultures contained similar levels of viral particles except cultures expressing TR310, TR314, and KAL010 (Fig. 3B, panel IV). The reduced expression of the packaging construct in these cultures correlated with the lower expression of the respective transfer vectors at the RNA level (Fig. 3B, panel II), suggesting that the lower expression of the transfer and packaging constructs was due to the lower transfection efficiency in these cultures.

Next, we analyzed the amount of RNA packaged by the virions produced in the transfected Cos cells. These analyses revealed that packaging was substantially reduced when only 30 bp of *gag* sequences were present in the transfer vector (see TR310, panel III, Fig. 3B). Quantitation of the amount of RNA packaged by TR310 revealed an approxi-

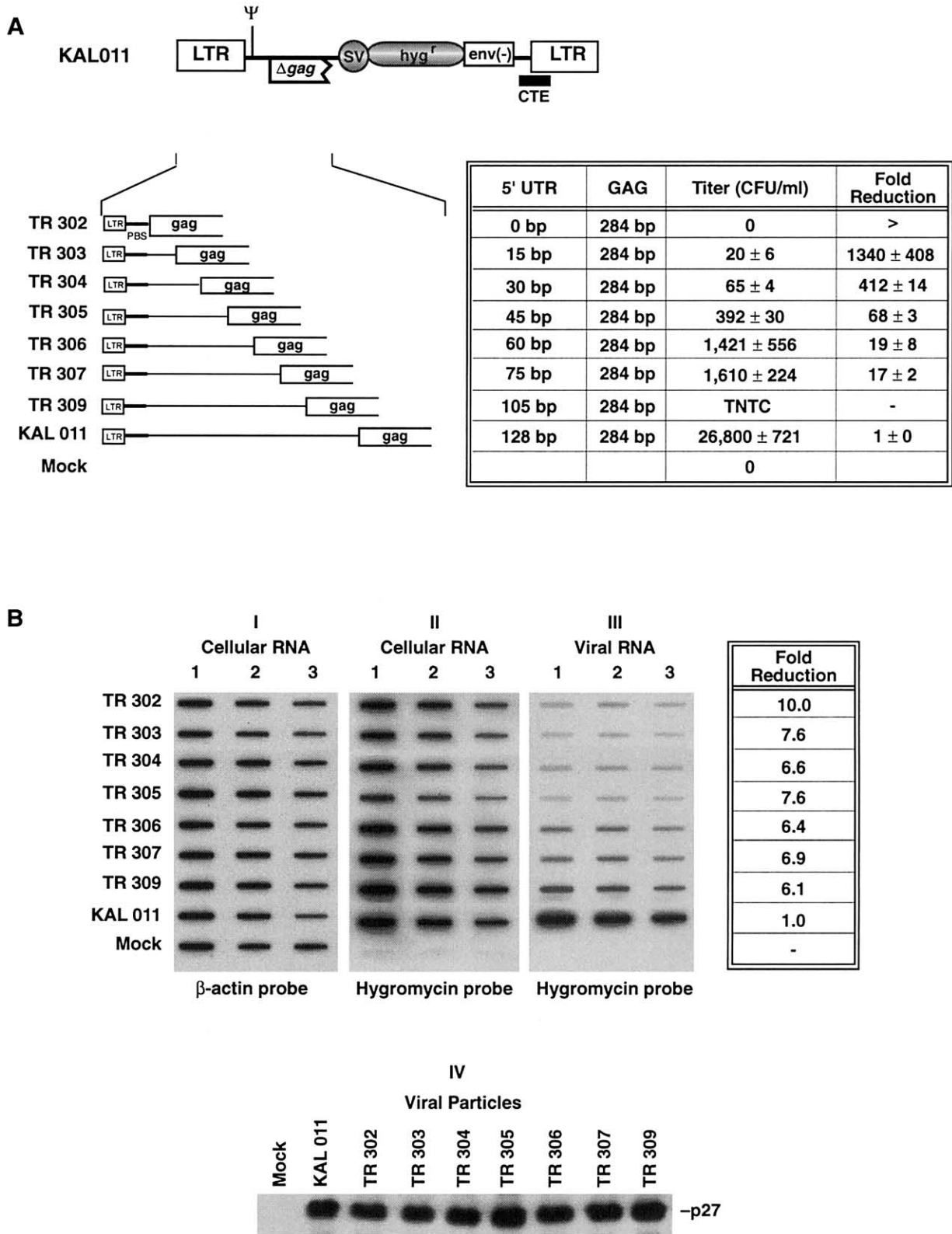


Fig. 2. The extreme ends of the 5' untranslated region (UTR) of MPMV are critical for efficient packaging of the MPMV genomic RNA in the presence of *gag*. (A) MPMV transfer vectors TR302–309 containing varying amounts of 5' UTR in the presence of 284 bp of *gag*. The virus titers obtained as colony-forming units per milliliter (CFU/ml) of virus stock posttransduction are indicated to the right along with the fold reduction in titers compared to KAL011. The value of each titer represents a mean of three independent experiments performed in duplicate along with the standard deviation. No hygromycin resistant (Hyg^r) colonies were observed for any of the transfer vectors or packaging and *env* expression constructs when transfected alone. >, essentially 100% reduction of viral titers; TNTC, too numerous to count. (B) RNA slot blot and Western blot analyses of virus particles and cellular RNAs

mately threefold loss in RNA packaged by the virions compared to KAL011 when normalized to the intracellular steady-state levels of transfer vectors RNAs (Fig. 3B, panels I–III). However, 100 bp of *gag* restored packaging efficiency to the same level as KAL011 (see TR311, Fig. 3B), and no further reductions in packaging efficiency were observed with the next four consecutive vectors that contained from 140 to 797 bp of *gag* (Fig. 3B). These results clearly demonstrate that 100 bp of *gag* are sufficient to confer efficient RNA packaging on the transfer vectors in the presence of the entire 5' UTR. In addition, these results also show that sequences within 797 bp of *gag* do not harbor any repressor sequences that affect RNA packaging negatively.

Test of TR310 to KAL010 in the *trans*-complementation assay revealed that the packaging efficiency observed with these vectors overall correlated well with the transduction efficiency after normalization of the viral titers with the amount of virus particles produced (see Materials and methods). These analyses revealed that presence of 30 bp of *gag* led to a fourfold loss in viral titers compared to KAL011 (Fig. 3A). It was not until the addition of 100 bp of *gag* that the transduction efficiency was restored to within twofold of KAL011 and remained within 1- to 2.5-fold of KAL011 with the remaining vectors that contained from 140 to 797 bp of *gag* (Fig. 3A). These results demonstrate that 100 bp of *gag* in the presence of the entire 5' UTR are sufficient not only for efficient packaging, but also for efficient transduction to the target cells.

MPMV contains a primary packaging determinant immediately downstream of the PBS whose function is affected by sequences at the 5' UTR/gag boundary

So far, the data presented in Figs. 2 and 3 have demonstrated that the first 15 bp immediately downstream of the PBS and the last 23 bp of the 5' UTR as well as the first 100 bp in *gag* are important for efficient RNA encapsidation in MPMV. However, the relative contribution and role of these sequences to packaging was not clear. Therefore, we analyzed the requirements of sequences within the 5' UTR and *gag* independently of one another. Toward this end, we generated another series of transfer vectors, TR315–323, that contained deletions in the 5' UTR in 15-bp increments, but in the absence of any *gag* sequences (Fig. 4A). These vectors were tested in the *in vivo* packaging and transduction assay as described before.

Slot blot analysis of RNA packaged from TR323 re-

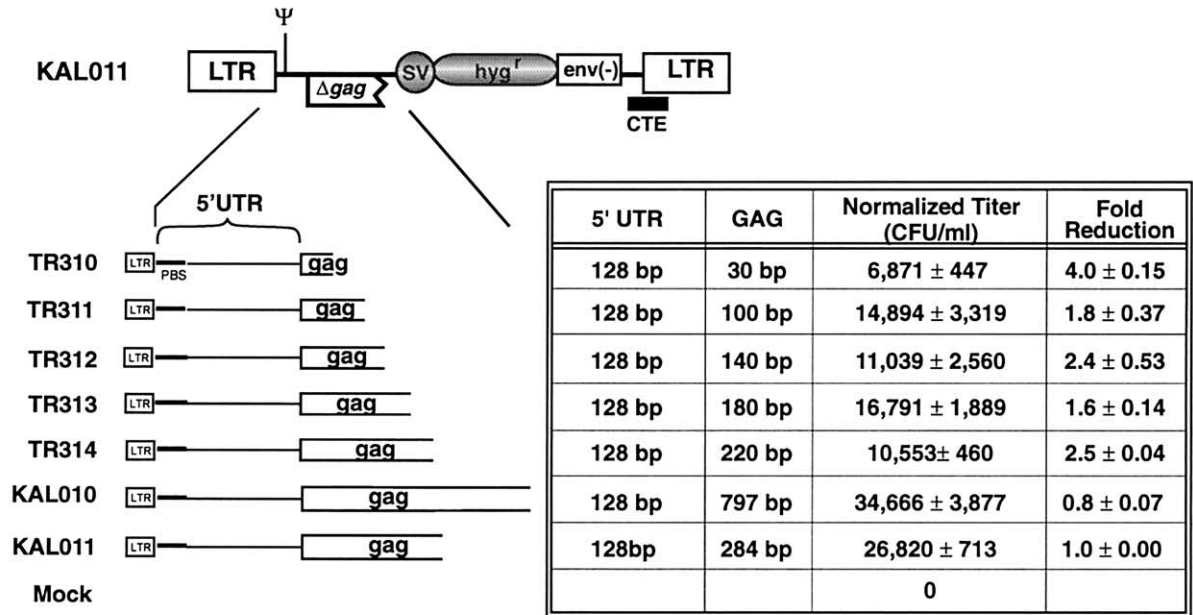
vealed that in the absence of *gag*, but in the presence of the entire 5' UTR, there was a 7.5-fold reduction in packaging efficiency compared to KAL011, after normalization with the intracellular steady-state levels of transfer vector RNAs (Fig. 4B, panels I–III). This suggested that sequences in *gag* affected packaging, as shown earlier (Fig. 3). A slightly improved packaging efficiency, in the absence of *gag*, was observed with the next two vectors that contained deletions of the last 23 and 38 bp of the 5' UTR, respectively (see TR321 and 322, Fig. 4B). This was unexpected since loss of the last 23 bp of the 5' UTR, in the presence of *gag*, had resulted in a 6.1-fold reduction in packaging efficiency (TR309, Fig. 2B). Interestingly, the packaging efficiency was restored essentially to that of KAL011 with further deletions of the next 45 bp (see TR318–319, Fig. 4B), and in fact, was enhanced somewhat by an additional 15 bp deletion in TR317 (Fig. 4B). This observation suggested that in the absence of *gag*, part or all of the sequences between 30 and 90 bp of the 5' UTR negatively affected the proper folding of the 5' UTR, while shortening of the region restored the folding potential such that the packaging signal could function efficiently. This inhibitory effect on the formation of the upstream packaging determinant was not apparent in the presence of *gag* sequences (Fig. 2). Thus, *gag* sequences seem to be important in stabilizing the formation of the upstream packaging determinant.

Further incremental deletions of 30 bp downstream of the PBS in the next two vectors resulted in the loss of packaging efficiency by nearly ninefold compared to KAL011 (see TR315 and 316, Fig. 4B). A similar observation was made with TR302 and TR303, vectors that contain the same 5' UTR deletions as TR315 and 316, but in the presence of *gag* in which the packaging efficiency was reduced by 10- and 7.6-fold, respectively, compared to KAL011 (Fig. 2B).

Together, results from the deletion analysis of the 5' UTR in the absence of *gag* sequences confirm our earlier observations that the two ends of the 5' UTR are important for efficient packaging in MPMV. The primary packaging determinant seems to reside within the 30 bp immediately downstream of the PBS, deletion of which maximally affects packaging efficiency. A complete restoration of the packaging efficiency in the absence of *gag* and the last 98 bp of the 5' UTR further reveals that the downstream sequences shown to affect packaging earlier (last 23 bp of the 5' UTR and 100 bp of *gag*) do not per se form the packaging signal, but probably affect the formation and/or

isolated from Cos cells transfected with the various transfer vectors along with the packaging (TR301) and *env* (MD.G) expression constructs from one representative experiment. The RNAs were DNase-treated, diluted, and subjected to slot blot analysis. Panel I represents a 1:2 dilution of 0.5 μg of cellular RNA (0.5, 0.25, and 0.125 μg) probed with a fragment of a housekeeping gene, β -actin, while panel II represents a 1:3 dilution of 2 μg of cellular RNA (2, 0.67, and 0.22 μg) probed with a fragment of the hygromycin gene. Panel III represents a 1:2 dilution of purified virion RNA isolated from the equivalent of a three-fourth portion of 9 ml media containing virus particles, also probed with a fragment of the hygromycin gene. The column to the right of panel III refers to the fold reduction in packaging efficiency relative to KAL011 after normalization for RNA loading and transfection efficiency. Panel IV shows Western blot analysis of equivalent amounts of the remaining one-fourth portion of the purified virions harvested from each of the transfected cultures in the corresponding *trans*-complementation assay using MPMV Gag/Pol polyclonal antiserum. Mock, cells transfected without DNA.

A



B

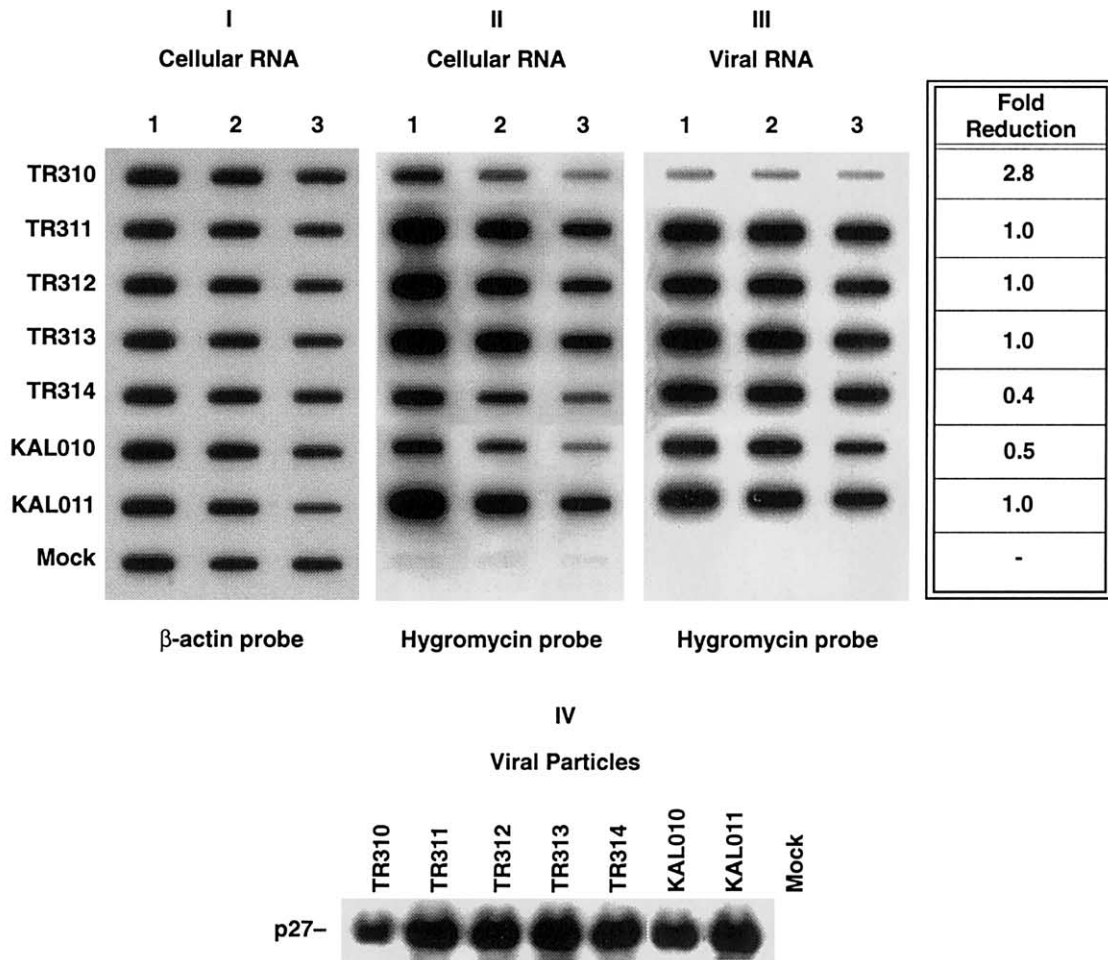


Fig. 3. The first 100 bp in *gag* are sufficient for efficient packaging of the MPMV genomic RNA in the presence of the entire 5' UTR. (A) MPMV transfer vectors TR310–314 containing varying amounts of *gag* sequences. The virus titers were obtained as colony-forming units per milliliter (CFU/ml) of virus

stability of the primary packaging determinant. Thus, simultaneous deletion of the primary and secondary determinants in TR315 (Fig. 4B) reduces the packaging efficiency to similar levels (ninefold) as deletion of the secondary determinant alone (TR323, 7.5-fold, Fig. 4B or TR302, 10-fold, Fig. 2B).

Finally, the transduction efficiency of TR315–323 was analyzed in the *in vivo* transduction assay. Once again, a progressive loss in transduction efficiency was observed with several incremental deletions in the 5' UTR. Presence of the entire 5' UTR in the absence of *gag* sequences resulted in a 36 ± 9 -fold loss in viral titers compared to KAL011 (TR323, Fig. 4A). There was another 10-fold drop in the transduction efficiency to 355 ± 50 -fold with a 23-bp deletion in the 5' UTR (TR322, Fig. 4A). Part of the decline in transduction efficiency observed could be attributable to the reduction in packaging efficiency (7.5- and 4.8-fold, respectively), while the remaining decline can be attributed to the loss of *cis*-acting elements by the deletions that affect vector RNA propagation.

With further incremental deletions of the subsequent 60 bp in the next four consecutive vectors, TR317–321, the drastic reduction in the transduction efficiency stabilized to between 410- and 578-fold compared to KAL011 (Fig. 4A). This is despite essentially wild-type levels of RNA packaging observed with these vectors except TR321. This suggested that sequences within 30–90 bp from the PBS (deleted in TR317–319) did not affect vector RNA propagation, while they negatively impacted RNA packaging in the absence of *gag* since their loss resulted in the return of the packaging efficiency back to the wild-type, as suggested earlier.

Once again, similar to TR303 and 304 (Fig. 2B), loss of sequences between 15 and 30 bp downstream from the PBS resulted in a further reduction in transduction efficiency from 578 ± 66 -fold in TR317 to 3900 ± 1110 in TR316 compared to KAL011 (~ a sevenfold drop), while no *Hyg*^r were observed with TR315, the vector that had lost the 15 bp immediately downstream from the PBS. The loss in titers observed with all the vectors was despite the fact that similar levels of virions were produced in each of the transfected cultures (Fig. 4B, panel IV). These data suggest that the extreme ends of the 5' UTR and beginning of *gag* harbor sequences that affect both RNA packaging and vector RNA propagation.

Discussion

This study used a systematic deletion analysis of the 5' UTR and *gag* sequences of MPMV to unravel the complex nature of its packaging determinants. Our results reveal that sequences important for MPMV packaging are found as two discrete elements, the first comprising 30 bp immediately downstream of the PBS, Region I (Fig. 2B), and the other comprising approximately the last 23 bp of the 5' UTR (Fig. 2B) and the first 100 bp of the *gag* gene, Region II (Fig. 3B). Our data further suggest that Region I serves as the primary packaging determinant of MPMV, while Region II is important for the formation and/or stability of the primary packaging determinant (Fig. 4B). This can be observed by the fact that Regions I and II were quite similar in their relative contribution toward packaging. Deletion of Region II (see TR309 in Fig. 2B and TR322 and 323 in Fig. 4B) resulted in a 5- to 7.5-fold (average ~6.25) drop in packaging efficiency compared to a complete deletion of both Regions I and II, which resulted in a similar 8.7- to 10-fold (average ~9.3) drop in packaging efficiency (see TR302 in Fig. 2B and TR315 in Fig. 4B). These findings are in contrast to what we have observed in FIV where of the two packaging determinants mapped; deletion of either one resulted in a 4- to 6-fold loss in packaging efficiency, while deletion of the two determinants together reduced packaging efficiency sharply to nearly 40-fold, suggesting synergistic effects of the two regions on packaging (Browning et al., 2003). Thus, the lack of synergy exhibited by MPMV packaging determinants versus those of FIV suggests differences in the manner in which the two viruses package their genomes.

These results are understandable given the high propensity of the 5' UTR and *gag* region of MPMV to fold into a complex higher order structure (Harrison et al., 1995). Based on this structure, Region I, encompassing 30 bp from the PBS, comaps with the first stem loop predicted by Harrison and colleagues. Similarly, sequences encompassing Region II has been predicted to fold into two stem loop structures. Our data also suggest that Region II may assume a higher order structure since deletion of *gag* sequences alone or the last 23 bp of the 5' UTR alone were sufficient to reduce the functionality of Region II for encapsidation (Figs. 2B and 4B).

As indicated earlier, we find that the region between the major SD and the Gag initiation codon (encompassed by the

stock posttransduction and were normalized to the virus particles produced as described under Materials and methods. The fold reduction in titers compared to KAL011 is indicated to the right. The raw values for each titer were obtained from a mean of three independent experiments performed in duplicate along with the standard deviation. (B) RNA slot blot and Western blot analyses of virus particles and cellular RNAs isolated from Cos cells transfected with the various transfer vectors as described in the legend to Fig. 2 from one representative experiment. Panels I and II are slot blots of cellular RNAs, while panel III is a slot blot of virion RNA isolated from transiently transfected Cos cells. The column to the right of panel III refers to the fold reduction in packaging efficiency relative to KAL011 after normalization for RNA loading and transfection efficiency. The RNAs were DNase treated and subjected to slot blot analysis as mentioned in the legend to Fig. 2. Panel IV shows Western blot analysis of purified virions harvested from each of the transfected cultures as described under Materials and methods. Mock, cells transfected without DNA.

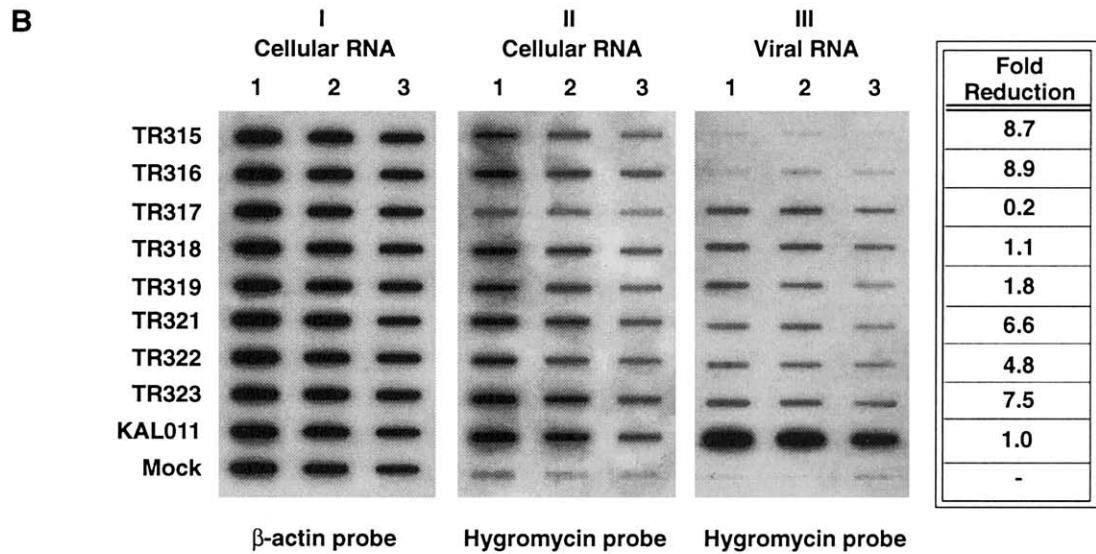
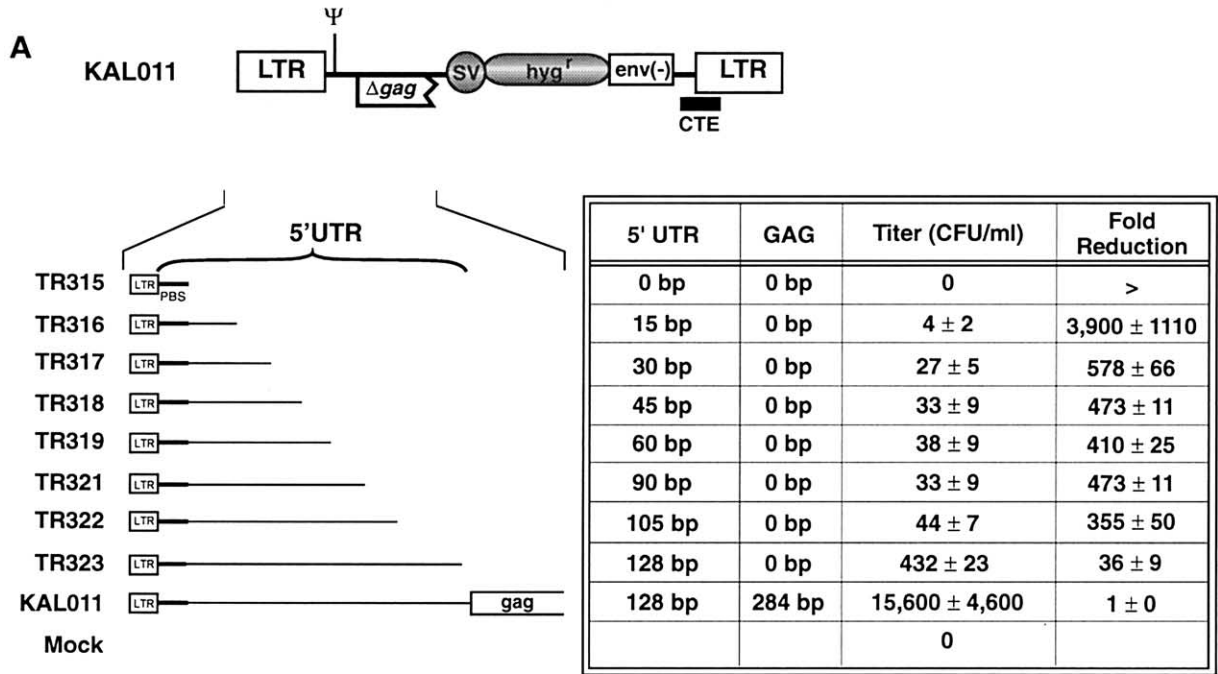


Fig. 4. The MPMV packaging signal is composed of two redundant packaging elements both of which are required for efficient RNA packaging. (A) Schematic representation of the MPMV transfer vectors TR315–323 containing varying amounts of 5' UTR in the absence of gag sequences. The virus titers obtained as colony-forming units per milliliter (CFU/ml) of virus stock posttransduction are indicated to the right along with the fold reduction in titers compared to KAL011. The value of each titer represents a mean of three independent experiments performed in duplicate along with the standard deviation. (B) RNA slot blot and Western blot analyses of virus particles and cellular RNAs isolated from Cos cells transfected with the various transfer constructs as

last 23 bp of the 5' UTR) is important for packaging (Fig. 2B). This is in contrast to the deletion analysis of Guesdon et al., who did not see a role of this region in packaging. According to their analysis, a 61-bp deletion upstream of the SD reduced MPMV RNA packaging by about twofold (58%), but not an 11-bp deletion downstream of the SD (Guesdon et al., 2001). The difference in the results of the two studies could be due to several reasons. One reason could be that, as our analysis indicates, the role of this region in packaging is more indirect, affecting the formation and/or stability of the primary packaging determinant located in Region I. Thus, the 11-bp deletion introduced by Guesdon et al. may not have been sufficiently large enough to have disrupted Region II and its ability to affect the packaging potential of the primary packaging determinant located in Region I. Another reason could be that Guesdon et al. used a replication-competent virus for the analysis of their deletion mutations. It is well known that use of a replication-competent virus leads to multiple rounds of replication that can mask effects of mutations that are not very pronounced or exaggerate the effects of mutations that may not be very significant. Our system used a single round of replication assay in which even minor effects of the mutation should be easily identifiable. In fact, our study indicates that the 61-bp deletion that Guesdon et al. found important in packaging is not essential for packaging in our system. Guesdon and colleagues have earlier predicted this 61-bp region to fold into the stable, conserved, stem loop 4 that contains a GC-rich stem that is found upstream of the SD (Harrison et al., 1995). In fact, site-directed mutagenesis designed to destabilize this stem loop in various ways or introduction of compensatory mutations to reform the mutated stem loop has also revealed that stem loop 4 does not seem to affect RNA packaging significantly in MPMV (Lew, K.A., Mustafa, F., Schmidt, R.D., Browning, M.T., and Rizvi, T.A., unpublished observations).

Our *trans*-complementation assay, in addition to assessing the role of the mutations on packaging, also provided information on the effect of these mutations on the ability of the vector RNAs to be propagated to the target cells. Analysis of the consequence of the deletions on vector RNA propagation revealed that overall loss in vector RNA titer was observed with each consecutive deletion in the 5' UTR. However, the terminal 23 bp of the 5' UTR and sequences near the PBS had a more dramatic effect than sequences within the middle region of the 5' UTR. Furthermore, the effect of these mutations on vector RNA propagation was more drastic in the absence of *gag* than in its presence (Figs. 2A and 4A). This suggests that *gag* sequences may have a

stabilizing role on 5' UTR sequences that affect vector RNA propagation. On the other hand, *gag* may also contain additional sequences that positively affect other steps of the retroviral life cycle.

In summary, a detailed deletion analysis of sequences within the 5' end of the MPMV genome reveals the presence of a primary packaging determinant immediately downstream of the PBS whose function is dependent upon the presence of sequences within the 5' UTR and the *gag* boundary. Information obtained from the analysis of these packaging determinants should be valuable in the development of improved retroviral vectors for the elucidation of basic steps in the replication of the type D retroviruses as well as the development of safer, more efficient retroviral vectors for gene therapy.

Materials and methods

Numbering system

Nucleotide designations for MPMV are based on GenBank Accession No. M12349.

Plasmid construction

MPMV packaging construct and envelope expression vector

The MPMV packaging construct TR301 has been described before (Browning et al., 2001) (Fig. 1A). TR301 expresses the *gag/pol* genes from the CMV/intron A/promoter/enhancer, contains MPMV CTE, and uses the BGH poly(A) sequences for transcript termination. The VSV-G envelope expression vector, MD.G, was obtained from Dr. Didier Trono and has been described before (Naldini et al., 1996) (Fig. 1B).

KAL010 and KAL011

KAL010 (Fig. 3B) and KAL011 (Fig. 1C) are MPMV transfer vectors constructed from KAL006 and KAL007 and contain 284 and 797 bp of *gag* gene downstream of the entire MPMV 5' UTR. KAL006 and KAL007 themselves were derived from the MPMV genomic construct, KAL001, that has been described before (Rizvi et al., 1996b). KAL006 contains MPMV sequences from the 5' LTR to nt 1687 of *gag*, while KAL007 contains MPMV sequences from the 5' LTR to nt 1172 of *gag*. At the 3' end, both KAL006 and KAL007 contain MPMV sequences from nt 7181 to the end of the 3' LTR. These plasmids were constructed by deleting all viral sequences between either nt

described in the legend to Fig. 2 from one representative experiment. Panels I and II are slot blots of cellular RNAs, while panel III is slot blot of virion RNA isolated from transiently transfected Cos cells. The column to the right of panel III refers to the fold reduction in packaging efficiency relative to KAL011 after normalization for RNA loading and transfection efficiency. The RNAs were DNase-treated, diluted, and subjected to slot blot analysis as mentioned in the legend to Fig. 2. Panel IV shows Western blot analysis of purified virions harvested from each of the transfected cultures as described under Materials and methods. Mock, cells transfected without DNA. *, sample lost.

1687 or nt 1172 and 7181, followed by a simultaneous insertion of a *NheI* linker at the point of deletion. A SV-Hyg^r cassette with flanking *NheI* sites was inserted in the correct orientation at the site of the *NheI* linker insertion to create KAL010 and KAL011, respectively.

5' UTR deletion vectors in the presence of gag sequences

TR302–309 (Fig. 2A) are MPMV transfer vectors that contain deletions in the 5' UTR in 15-bp increments from the start of *gag* to the end of the PBS in the presence of 284 bp of *gag* sequences. These vectors were generated via PCR amplification of fragments of the 5' UTR using a derivative of KAL001, KAL048, as a template. KAL048 is a MPMV transfer vector that contains all viral sequences other than a deletion at the 3' end of the viral genome encompassing the end of *env* and the MPMV CTE (Rizvi et al., 1996b). The PCR used sense (S) oligonucleotide OpIC19H (ATGAC-CATGATTAcgccaag) that corresponds to sequences upstream of the 5' UTR in the cloning vector pIC19H that was used to create KAL048 and individual antisense (A) oligonucleotides listed below (uppercase for MPMV sequences while lowercase for *NheI* site introduced for cloning purposes):

- TR302 OTR184 (AS; 5' cccgctagcGCCCCAGCTTGGGCG 3'; nt 761–747)
 TR303 OTR185 (AS; 5' cccgctagcATTCCTCGTATCCA 3'; nt 776–762)
 TR304 OTR186 (AS; 5' cccgctagcCGTCTTCCTCACGAA 3'; nt 791–777)
 TR305 OTR187 (AS; 5' cccgctagcGGCCGGCGAACGCGT 3'; nt 806–792)
 TR306 OTR188 (AS 5' cccgctagcTCACTTTTAATCGCC 3', nt 821–807)
 TR307 OTR189 (AS 5' cccgctagcCAAGAGAGTTTACTT 3', nt 836–837)
 TR308 OTR 190 (AS 5' cccgctagcGGTTCCCGCGGCGGC 3', nt 851–837)
 TR309 OTR191 (AS 5' cccgctagcAGGTCCAACGCGCA 3', nt 866–852)

The PCR products were digested with *SalI* and *NheI* and cloned into the *XhoI* and *NheI* sites of KAL011, creating subclones that lacked any *gag* sequences, the SV-Hyg^r cassette, or CTE. Next, KAL007 was used as the template to reintroduce MPMV *gag* sequences between 890 and 1172 and *env* sequences between 7181 and 7578 by PCR using oligonucleotides OTR195 (S; 5' ggactagtATGGGGCAAGAATTAAGC 3'; nt 890–907) and OTR144 (AS; 5' ACGGCTCCGGACATGAGATCTTGTATAGTGCTA GAA 3'; nt 8219–8205 followed by nt 7578–7558). The PCR products were digested with *SpeI* and *BglII* and ligated to the *NheI* and *BglII* sites of the subclones. Finally, the SV-Hyg^r cassette was reinserted at the *NheI* site created by PCR downstream of the *gag* sequences to generate TR302–309.

MPMV transfer vectors with incremental insertions of gag to the 5' UTR

TR310–314 are MPMV transfer vectors that contain the entire 5' UTR juxtaposed to varying amounts of *gag* sequences from 0 to 220 bp. These vectors were created in a manner very similar to the above vectors except that the entire 5' UTR was amplified along with incremental additions of *gag*. The PCR was performed as before using KAL048 as the template and OpIC19H as the sense oligonucleotide, while the antisense oligonucleotides used were as follows:

- TR310 OTR193 (AS; 5' cccgctagcAACGTTTCATGCTGGC 3'; nt 920–906)
 TR311 OTR196 (AS; 5' cccgctagcAATTTCAAAAAGATCA 3'; nt 990–976)
 TR312 OTR197 (AS; 5' cccgctagcTTGCGGAAACCAAGG 3'; nt 1030–1016)
 TR313 OTR198 (AS; 5' cccgctagcCGCCTACTCGACGCC 3'; nt 1070–1056)
 TR314 OTR199 (AS; 5' cccgctagcTTCTCCGGGCCAAAA 3'; nt 1110–1096)

The PCR fragments obtained were digested and cloned using the several stages of cloning as described above to generate the final constructs.

5' UTR deletion vectors in the absence of gag sequences

TR315–323 are MPMV transfer vectors that contain the same 5' UTR deletions described for TR302–309, but in the absence of *gag* sequences. The deletions were created by PCR using the sense oligonucleotide OpIC19H and antisense oligonucleotides OTR185–191 as described above and KAL048 as the template. The PCR products were digested with *SalI* and *NheI* and cloned into the *XhoI* and *NheI* sites of KAL011 as before with the reinsertion of the SV-Hyg^r cassette at the *NheI* site, creating the final vectors.

All PCR amplifications were performed using the Perkin-Elmer 9600 thermocycler with MicroAmp tubes as described before (Browning et al., 2001).

Transfections and infections of cells

Cos cells were maintained at 37°C in Dulbecco's modified Eagle's medium (DMEM) supplemented with 10% fetal bovine serum from Hyclone (Logan, UT). HeLa CD4⁺ cells were maintained in DMEM supplemented with 7% calf serum from Hyclone. Transfections of Cos cells and infections of HeLa CD4⁺ cells have been described before (Browning et al., 2001).

Western and slot blot analyses

Virus particles were harvested from 9 ml of clarified tissue culture supernatants as described earlier (Browning et al., 2001). Virus particles were resuspended in 100 µl of TNE buffer (50 mM Tris-Cl, pH 7.4, 100 mM NaCl, and 1

mM EDTA, pH 8.0) of which 25 μ l was used for protein extraction, while the remaining 75 μ l was used to isolate virion RNA. Viral proteins were analyzed by Western blot analysis using the Enhanced Chemiluminescence kit (Amersham, Arlington Heights, IL) as described before (Rizvi et al., 1997). The anti-MPMV Gag/Pol Pr78 polyserum was kindly provided by Dr. Eric Hunter (University of Alabama, Birmingham, AL).

Viral RNA was isolated from the pelleted viral particles and transfected Cos cells as described before (Browning et al., 2001). Both viral and cellular RNAs were treated with RNase-free DNase to eliminate any contaminating DNA and blotted on slot blots for analysis as described before (Rizvi et al., 1996b, 1997). The filters were hybridized with either a *hygromycin* gene-specific DNA probe or a β -actin cDNA probe (Clontech, Palo Alto, CA) as described earlier (Rizvi et al., 1996b).

Normalization of packaging and transduction efficiencies

Normalization of packaging efficiency was performed briefly as follows: band intensities in the slot blots were estimated by scanning the autoradiographs electronically and using the Multi Analyst software (version 1.1) from Bio-Rad Laboratories (Hercules, CA) for measuring optical densities. Background densities observed in mock transfections were first subtracted from test values followed by normalization of each value with the background-subtracted values obtained from the control vector, KAL011. Subsequently, values obtained from the three dilutions of each RNA sample were averaged and the packaging efficiency determined as follows:

$$\text{Packaging Efficiency} = \frac{A}{B \times C}$$

where A = average of amount of RNA packaged into virions, as observed in panel III of slot blots (after subtraction of background and normalization with KAL011), B = average of amount of cellular RNA loaded, as observed in panel I of slot blots (after normalization with KAL011), and C = average of amount of transfer vector RNA expressed, as observed in panel II of slot blots (after subtraction of background and normalization with KAL011).

Finally, the fold reduction in packaging efficiency was obtained by dividing the packaging efficiency obtained for each construct with that of KAL011.

Similarly, in Fig. 3, viral titers were normalized to the amount of particles produced by first measuring the optical densities observed in the Western blots of virus particles and dividing with that observed for KAL011 after subtraction of background. Next, the titers observed were divided by the factor obtained to calculate the normalized viral titers. Finally, fold reduction in viral titers was obtained by dividing the normalized viral titers with that observed for KAL011.

Acknowledgments

We express our sincere thanks to Judy T. Ing (University of Texas M.D. Anderson Cancer Center, Research Division, Science Park, Smithville, TX) for excellent help with the graphics. We acknowledge Dr. Didier Trono (Salk Institute, La Jolla, CA) for MD.G, Dr. Eric Hunter (University of Alabama, Birmingham, AL) for providing MPMV molecular clone pSHRM15 and MPMV Gag/Pol polyclonal serum, and Dr. Mary-Louise Hammarskjold (University of Virginia, Charlottesville, VA) for providing MPMV CTE. This work was supported, in part, by funds from the American Heart Association (AHA 9950182N) and the Faculty of Medicine and Health Sciences (FMHS), UAE University (New Project Grant 2002-NP/02/30).

References

- Adam, M.A., Miller, A.D., 1988. Identification of a signal in murine retrovirus that is sufficient for packaging of nonretroviral RNA into virions. *J. Virol.* 62, 3802–3806.
- Akkina, R.K., Walton, R.M., Chen, M.L., Li, Q.X., Planelles, V., Chen, I.S.Y., 1996. High efficiency gene transfer into CD34(+) cells with a human immunodeficiency virus type 1-based retroviral vector pseudotyped with vesicular stomatitis virus envelope glycoprotein. *G. J. Virol.* 70, 2581–2585.
- Albritton, L.M., Tseng, L., Scadden, D., Cunningham, J.M., 1989. A putative murine ecotropic retrovirus receptor gene encodes a multiple membrane spanning protein and confers susceptibility to virus infection. *Cell* 57, 659–666.
- Arnoff, R., Hajjar, A.M., Linial, M.L., 1993. Avian retroviral RNA encapsidation: reexamination of functional 5' RNA sequences and the role of nucleocapsid Cys-His motifs. *J. Virol.* 67, 178–188.
- Banks, J.D., Linial, M.L., 2000. Secondary structure analysis of a minimal avian leucosis-sarcoma virus packaging signal. *J. Virol.* 74, 456–464.
- Banks, J.D., Yeo, A., Green, K., Cepeda, F., Linial, M.L., 1998. A minimal avian retroviral packaging sequence has a complex structure. *J. Virol.* 72, 6190–6194.
- Bender, M.A., Palmer, T.D., Galinas, R.E., Miller, A.D., 1987. Evidence that the packaging signal of Moloney murine leukemia virus extends into the gag region. *J. Virol.* 61, 1639–1646.
- Browning, M.T., Schmidt, R.D., Lew, K.A., Rizvi, T.A., 2001. Primate and feline lentiviral vector RNA packaging and propagation by heterologous lentiviral virions. *J. Virol.* 75, 5129–5140.
- Browning, M.T., Mustafa, F., Schmidt, R.D., Lew, K.A., Rizvi, T.A., 2003. Delineation of sequences important for efficient FIV RNA packaging. *J. Gen. Virol.*, in press.
- Bryant, M.L., Gardner, M.B., Marx, P.A., Maul, D.H., Lerche, N.W., Osborn, K.J., Lowenstine, L.J., Bogden, A., Arthur, L.O., Hunter, E., 1986. Immunodeficiency in rhesus monkeys associated with the original Mason-Pfizer monkey virus. *J. Natl. Cancer Inst.* 77, 957–965.
- Daniel, M.D., King, N.W., Letvin, N.L., Hunt, R.D., Sehgal, P.K., Desrosiers, R.C., 1984. A new type D retrovirus isolated from macaques with an immunodeficiency syndrome. *Science* 223, 602–605.
- De Guzman, R.N., Wu, Z.R., Stalling, C.C., Pappalardo, L., Borer, P.N., Summers, M.F., 1998. Structure of the HIV-1 nucleocapsid protein bound to the SL3 ψ -RNA recognition element. *Science* 279, 384–388.
- Desrosiers, R.C., Daniel, M.D., Butler, C.V., Schmidt, D.K., Letvin, N.L., Hunt, R.D., King, N.W., Barker, C.S., Hunter, E., 1985. Retrovirus D/New England and its relation to Mason-Pfizer monkey virus. *J. Virol.* 54, 552–560.

- Fine, D.L., Landon, J.C., Pienta, R.J., Kubicek, M.T., Valerio, M.J., Loeb, W.F., Chopra, H.C., 1975. Responses of infant rhesus monkeys to inoculation with Mason-Pfizer monkey virus. *J. Natl. Cancer Inst.* 54, 651–658.
- Guesdon, F.M.J., Gretores, J., Rhee, S.R., Fisher, R., Hunter, E., Lever, A.M.L., 2001. Sequences in the 5' leader of Mason-Pfizer monkey virus which affect viral particle production and genomic RNA packaging: development of MPMV packaging cell lines. *Virology* 288, 81–88, doi:10.1006/viro.2001.1061.
- Gunzburg, W.H., Saller, R.M., Salmoms, B., 1995. Retroviral vectors directed to predefined cell types for gene therapy. *Biologicals* 23, 5–12.
- Harrison, G.P., Hunter, E., Lever, A.M.L., 1995. Secondary structure model of the Mason-Pfizer monkey virus 5' leader sequence: identification of a structural motif common to a variety of retroviruses. *J. Virol.* 69, 2175–2186.
- Katz, R.A., Terry, R.W., Skalka, A.M., 1986. A conserved *cis*-acting sequence in the 5' leader of avian sarcoma virus RNA is required for packaging. *J. Virol.* 59, 163–167.
- Kaye, J.F., Lever, A.M.L., 1999. Human immunodeficiency virus types 1 and 2 differ in the predominant mechanism used for selection of genomic RNA for encapsidation. *J. Virol.* 73, 3023–3031.
- Lee, B.M., DeGuzman, R.N., Turner, B.G., Tjandra, N., Summers, M.F., 1998. Dynamic behavior of the HIV-1 nucleocapsid protein. *J. Mol. Biol.* 279, 633–649.
- Lever, A.M.L., 2000. HIV RNA packaging and lentivirus-based vectors. *Adv. Pharmacol.* 48, 1–28.
- Li, B., Nguyen, S., Li, X., Machida, C.A., 2001. Simian retrovirus vectors for gene transfer in nonhuman primate cells. *Virus Res.* 75, 155–168.
- Linial, M.L., Miller, A.D., 1990. Retroviral RNA packaging: sequence requirements and implications. *Curr. Top. Microbiol. Immunol.* 157, 125–152.
- Mann, R.R., Mulligan, R.C., Baltimore, D., 1983. Construction of a retrovirus packaging mutant and its use to produce helper-free defective retrovirus. *Cell* 33, 153–159.
- Mansky, L.M., Wisniewski, R.M., 1998. The bovine leukemia virus encapsidation signal is composed of RNA secondary structures. *J. Virol.* 72, 3196–3204.
- Marx, P.A., Maul, D.H., Osborn, K.G., Lerche, N.W., Moody, P., et al., 1984. Simian AIDS: isolation of a type D retrovirus and transmission of the disease. *Science* 223, 1083–1086.
- McBride, M.S., Panganiban, A.T., 1996. The human immunodeficiency virus type 1 encapsidation site is a multipartite RNA element composed of functional hairpin structures. *J. Virol.* 70, 2963–2973.
- McBride, M.S., Panganiban, A.T., 1997. Position dependence of functional hairpins important for human immunodeficiency virus type 1 encapsidation in vivo. *J. Virol.* 71, 2050–2058.
- McCann, E.M., Lever, A.M.L., 1997. Location of *cis*-acting signals important for RNA encapsidation in the leader sequence of human immunodeficiency virus type 2. *J. Virol.* 71, 4133–4137.
- Mitrophanous, K.A., Yoon, S., Rohll, J.B., Patil, D., Wilkes, F.J., Kim, V.N., Kingsman, S.M., Kingsman, A.M., Mazarakis, N.D., 1999. Stable gene transfer to the nervous system using a non-primate lentiviral vector. *Gene Ther.* 6, 1808–1818.
- Naldini, L., Blomer, U., Gally, P., Ory, D., Mulligan, R., Gage, F.H., Verma, I.M., Trono, D., 1996. *In vivo* gene delivery and stable transduction of nondividing cells by a lentiviral vector. *Science* 272, 263–267.
- Panganiban, A.T., Fiore, D., 1988. Ordered interstrand and intrastrand DNA transfer during reverse transcription. *Science* 241, 1064–1069.
- Rizvi, T.A., Panganiban, A.T., 1993. Simian immunodeficiency virus RNA is efficiently encapsidated by human immunodeficiency virus type 1 particles. *J. Virol.* 67, 2681–2688.
- Rizvi, T.A., Lew, K.A., Murphy Jr., E.C., Schmidt, R.D., 1996b. Role of Mason-Pfizer monkey virus (MPMV) constitutive transport element (CTE) in the propagation of MPMV vectors by genetic complementation using homologous/heterologous *env* genes. *Virology* 224, 517–532.
- Rizvi, T.A., Schmidt, R.D., Lew, K.A., 1997. Mason-Pfizer monkey virus (MPMV) constitutive transport element (CTE) functions in a position-dependent manner. *Virology* 236, 118–129.
- Rizvi, T.A., Schmidt, R.D., Lew, K.A., Keeling, M.E., 1996a. Rev/RRE-independent Mason-Pfizer monkey virus-constitutive transport element-dependent propagation of SIVmac239 vectors using a single round of replication assay. *Virology* 222, 457–463.
- Rosenberg, S.A., Aebersold, P., Cornetta, K., Kasid, A., Morgan, R.A., Moen, R., Karson, E.M., Lotze, M.T., Yang, J.C., Topalian, S.L., et al., 1990. Gene transfer into humans—immunotherapy of patients with advanced melanoma, using tumor-infiltrating lymphocytes modified by retroviral gene transduction. *N. Eng. J. Med.* 323, 570–578.
- Swanstrom, R., Wills, J.W., 1997. Synthesis, assembly, and processing of viral proteins, in: Coffin, J.M., Hughes, S.H., Varmus, H.E. (Eds.), *Retroviruses*, Cold Spring Harbor Laboratory Press, New York, pp. 289–294.
- Takeuchi, Y., Vile, R.G., Simpson, G., O'Hara, B., Collins, M.K., Weiss, R.A., 1992. Feline leukemia virus subgroup B uses the same cell surface receptor as gibbon ape leukemia virus. *J. Virol.* 66, 1219–1222.
- Temin, H.M., 1989. Retrovirus vectors: promise and reality. *Science* 246, 983.
- Vile, R.G., Ali, M., Hunter, E., McClure, M.O., 1992. Identification of a generalized packaging sequence for D-type retroviruses and generation of a D-type retroviral vector. *Virology* 189, 786–791.
- Watanabe, S., Temin, H.M., 1982. Encapsidation sequences for spleen necrosis virus, an avian retrovirus, are between the 5' long terminal repeat and the start of the *gag* gene. *Proc. Natl. Acad. Sci. USA* 79, 5986–5990.